Chicken Liver Bile Acid-Binding Protein Is in a Compact Partly Folded State at Acidic pH. Its Relevance to the Interaction with Lipid Membranes†

Verónica Nolan,‡ Massimiliano Perduca,‖ Hugo L. Monaco,‖ and Guillermo G. Montich*,‡

Departamento de Química Biológica, Facultad de Ciencias Químicas, Universidad Nacional de Córdoba - CIQUIBIC (CONICET) - Pabellón Argentina, Ciudad Universitaria (5000) Córdoba, Argentina, and Laboratorio di Biocristallografia, Dipartimento Scientifico e Tecnologico, Università di Verona, Italia

Received January 21, 2005; Revised Manuscript Received April 16, 2005

ABSTRACT: Chicken liver bile acid-binding protein (formerly known as chicken liver basic fatty acid-binding protein) binds to anionic lipid membranes acquiring a partly folded state [Nolan, V., Perduca, M., Monaco, H., Maggio, B., and Montich, G. (2003) *Biochim. Biophys. Acta 1611*, 98−106]. To understand the mechanisms of its interactions with membranes, we have investigated the presence of partly folded states in solution. Using fluorescence spectroscopy of the single Trp residue, circular dichroism in the far- and near-UV, Fourier transform infrared spectroscopy, and size-exclusion chromatography, we found that L-BABP was partly unfolded at pH 2.5 and low ionic strength, retaining some of its secondary structure. Addition of 0.1 M NaCl at pH 2.5 or decreasing the pH to 1.5 produced a more compact partly folded state, with a partial increase of secondary structure and none of tertiary structure. Fluorescence emission spectra of this state indicate that the Trp residue is within an environment of low polarity, similar to the native state. This environment is not produced by the insertion of the Trp into soluble aggregates as revealed by size-exclusion chromatography, fluorescence anisotropy, and infrared spectroscopy. The presence of partly folded states under acidic conditions in solution suggests the possibility that membrane binding of L-BABP occurs via this state.

Chicken liver bile acid-binding protein (L-BABP)[1], formerly called liver "basic" fatty acid-binding protein, (Lb-FABP) belongs to a family of low molecular mass proteins (14−15 kDa) that bind fatty acids and other nonpolar ligands (*1*). Recent work on the structure of its cocrystals with cholate, as well as an analysis of its sequence similarity with other members of the BABP family, supports the proposal that its function is most likely that of bile acid rather than fatty acid transport (*2*). Its three-dimensional structure is typical of the entire protein family, that is, a β-barrel consisting of 10 antiparallel β-strands arranged in two orthogonal β-sheets enclosing an inner cavity where the ligand is bound (*2*).

Several alternative roles have been proposed for the other members of this protein family, mostly called fatty acid or lipid-binding proteins (FABPs): to facilitate the solubilization and transport of ligands to be utilized by the metabolic machinery of the cell (*3*), to store fatty acids, to modulate their inhibitory effects and those of their CoA derivatives on specific enzyme systems (*4*), and also to protect the cell from the detergent effect of free fatty acids. Because these proteins are proposed to be involved in transferring nonpolar compounds between cell compartments and organelles, the interactions that they can establish with lipid membranes are relevant to their physiological role. Previous studies of the interaction of several FABPs with lipid vesicles of controlled composition have shown that FABPs can transfer fluorescent nonpolar compounds to lipid membranes by releasing the ligand into the aqueous phase (*5*) or by direct collision with the interface (*6*). The transient interactions that these proteins establish with the membrane must play a key role in both mechanisms.

Recently, we found that chicken L-BABP (that we called at the time liver "basic" FABP, Lb-FABP) binds to lipid membranes of the anionic lipid phosphatidylglycerol when the aqueous medium contains low amounts of salt. At high ionic strength, no binding to the zwiterionic lipid phosphatidylcholine nor to the anionic lipid was detected which indicates that the binding is driven mainly by electrostatic forces. The membrane-bound L-BABP presents large changes in the amide I′ infrared spectra as compared to the native protein in solution. An increase in the relative proportion of turns and unordered structures and a decrease in β-sheet components account for these changes. The conformational change of the membrane-bound protein does not correspond to a global unfolding of the protein in the membrane (*7*). The bound protein can be released by increasing the ionic

† This work was supported by grants from CONICET, SECYT-UNC, FONCYT, and Agencia Córdoba Ciencia. The Biocrystallography laboratory of the University of Verona is funded by a grant from the Italian Ministry of Education and Scientific Research. V.N. is a CONICET fellow and G.G.M. is a CONICET research officer.

* Corresponding author. Phone, +54 351 4334168; fax, +54 351 4334074; e-mail, gmontich@dqb.fcq.unc.edu.ar.

‡ Universidad Nacional de Córdoba.

‖ Università di Verona.

[1] Abbreviations: L-BABP, liver bile acid-binding protein; Lb-FABP, chicken liver basic fatty acid-binding protein; FABPs, fatty acid-binding proteins; BABP, bile acid-binding protein; FTIR, Fourier transform infrared spectroscopy; IR, infrared; CD, circular dichroism; GuHCl, guanidine hydrochloride; fwhh, full width at half-height; Rs, Stokes radius; *M*, molecular mass.

10.1021/bi050129r CCC: $30.25
Published on Web 05/17/2005

strength of the medium, and the native structure is largely recovered. We have proposed that the membrane-bound L-BABP has the characteristics of a partly folded state. This observation raises the question of whether a folding intermediate, already present in solution, binds to the membrane or whether the native protein binds to the membrane and then the conformational change is induced by the lipids. A similar question has been answered for cytochrome *c*; Pinheiro et al. showed that a folding intermediate present in solution is the species that interacts with membranes (*8*) and that its rate of unfolding is dramatically increased by the interaction with the membrane. Similar information is not available for chicken L-BABP. The identification of folding intermediates in solution could help to understand the mechanisms of interaction with lipid membranes.

Our previous studies regarding the interactions of L-BABP with lipid membranes were done with a protein that contained the heterogeneous population of endogenous ligands that is found in the protein purified from its natural source (*7*). In the present work, we study the solution properties of apo L-BABP. We used circular dichroism in the far- and near-UV region to investigate the presence of stable secondary and tertiary structure, respectively. Secondary structure was also evaluated by Fourier transform infrared (FTIR) spectroscopy. Conformational changes were also studied by fluorescence spectroscopy of the single Trp residue in L-BABP. The compactness and degree of aggregation were studied with size-exclusion chromatography. We found that chicken L-BABP acquires compact, partly folded states in solution under acidic conditions. These states contain a large proportion of secondary structure, and apparently, the amount of α-helix is increased as compared with the native structure. These partly folded intermediates can be relevant to understand the mechanism of interaction with lipid membranes.

MATERIALS AND METHODS

Materials. Apo chicken L-BABP was purified according to Scapin et al. (*9*) and stored in buffered aqueous solution (pH = 7.5) at −70 °C. NaCl, NaOH, HCl, NaOD, DCl, Tris (tris(hydroxymethyl)aminomethane) glycine, Sephadex G-75, and guanidine hydrochloride (GuHCl) were from Sigma (St. Louis, MO).

Sample Preparation for Fluorescence Spectroscopy, Circular Dichroism, and Gel Filtration Assays. Small volumes of stock solutions of L-BABP in aqueous solution were added to buffers at the desired pH and ionic strength. The samples were incubated 4 h at 25 °C, and the pH values were measured before the spectroscopy measurements or chromatography assays. Buffer solutions contained 10 mM glycine at pH between 1 and 3, 10 mM acetate−acetic buffer at pH between 4 and 6, and 10 mM Tris at pH 7. The pH was measured with a glass combination microelectrode MI-410 from Microelectrodes (Bedford, NH). The high ionic strength buffer contained 0.1 M NaCl.

Size-Exclusion Chromatography. A Sephadex G-75 column (0.5 mm × 20 mm) was equilibrated with buffer at the desired pH and ionic strength. Once the column was equilibrated, 100 μL of a sample containing apo L-BABP at the desired condition was loaded. The flow rate was 0.5 mL/min. The UV absorbance of the column output was continuously monitored. The protein distribution coefficients, K_d, were calculated according to $K_d = (V_e - V_0)/V_s$, where V_e is the protein elution volume, V_0 is the void volume, and V_s is the volume of the stationary phase. V_0 and V_s were not altered by changes in the pH and ionic strength. The column was calibrated at pH = 7 with carbonic anhydrase (30 kDa), myoglobin (17 kDa), and lysozyme (14 kDa). To study the hydrodynamic behavior of unfolded L-BABP in 10 mM Tris, 0.1 M NaCl, and 6 M GuHCl, pH 7.0, we used a Spharose-12 column and a fast-protein liquid chromatography system (Pharmacia, Uppsala, Sweeden). The Sepharose-12 column was calibrated with bovine serum albumin (66 kDa) and α-lactalbumin (14 kDa) in the absence of GuHCl.

Fluorescence Spectroscopy. Fluorescence spectra were recorded in a SLM 4800C spectrofluorometer. A quartz cell with 3 mm path length and a thermostatized holder was used. The slits were set at 4 nm for acquisition of fluorescence emission spectra, and the Trp residue was selectively excited at 290 nm. For fluorescence anisotropy measurements, the emission slits were set at 16 nm. The Raman contribution from water was subtracted from all spectra. Trp fluorescence anisotropy was measured at 320 nm for the native protein and at 340 nm for the blue-shifted spectra (see results) and calculated according to $r = (I_{VV} - GI_{VH})/(I_{VV} + (2GI_{VH}))$, where $G = I_{HV}/I_{HH}$, (*10*), I is the intensity, and the first and second subscripts refer to the plane of polarization of the excitation and emission beams, that is, V, vertical and H, horizontal. The solutions contained 7 μM protein for the acquisition of emission spectra and 20 μM for anisotropy measurements.

Circular Dichroism. Far-UV−CD. The measurements were made with a Jasco J-810 spectropolarimeter using a 0.2-cm path length quartz cell. Each spectrum was an average of six scans. The protein concentration used was 7 μM. The contribution of the buffer was subtracted in all spectra. Scan speed was set at 50 nm/min, with a 2-s response time, 0.2-nm data pitch, and 2-nm bandwidth. Molar ellipticity was calculated according to

$$[\theta]_\lambda^{MRW} = \text{MRW}\ \theta/lc$$

where MRW is the mean residue molecular weight calculated from the protein sequence, θ is the measured ellipticity (in degrees) at a given wavelength, l is the cuvette path length in mm, and c is the protein concentration in g/mL. Measurements were carried out in the 190−260 nm region.

Near-UV−CD. Measurements were made using a 1-cm path length quartz cell. Each spectrum was an average of six scans. The protein concentration was 150 μM for pH 7, 4, and 1.5 and 75 μM for pH 2 with and without salt. The contribution of the buffer was subtracted in all spectra. Scan speed was set at 50 nm/min, with a 2-s response time, 0.2-nm data pitch, and 2-nm bandwidth. Measurements were carried out in the 240−320 nm region.

FTIR Spectroscopy and Sample Preparation. Spectra were recorded in a Nicolet-Nexus spectrometer using a cell for liquid samples with CaF_2 windows and 75-μm Teflon spacers. The spectrometer was flushed with dry air to reduce water vapor distortions in the spectra. Five hundred scans were collected both for the background and the sample at a nominal resolution of 2 cm^{-1}. For sample preparation, 0.1 mg of lyophilized protein was resuspended with 30 μL of a D_2O solution at the desired pD and ionic strength, and

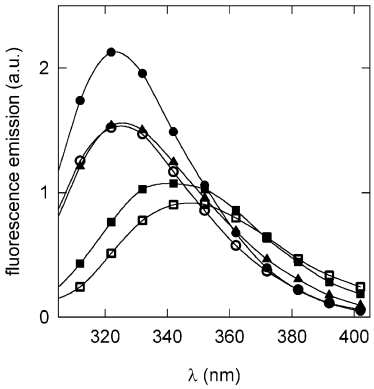

FIGURE 1: Fluorescence emission spectra of L-BABP at different pHs and salt conditions. (●) pH 7; (■) pH 2.4 no salt added; (○) pH 1.6; (▲) pH 2.4 and 0.1 M NaCl; and (□) pH 7 and 2 M GuHCl. Symbols are used for identification purposes and do not represent individual data points.

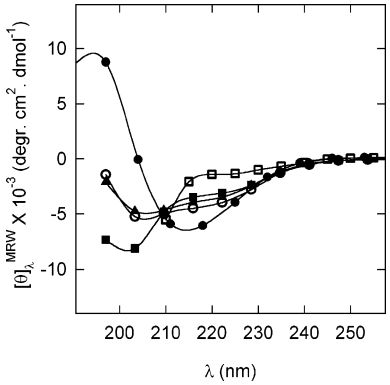

FIGURE 2: Far-UV−CD spectra of L-BABP at different pHs and salt conditions. (●) pH 7; (■) pH 2.4 no salt added; (○) pH 1.6; (▲) pH 2.4 and 0.1 M NaCl; and (□) pH 7 and 2 M GuHCl. Symbols are used for identification purposes and do not represent individual data points.

incubated for 24 h at room temperature to allow deuterium exchange of the amide protons. The pD of the sample was controlled after measuring.

All the measurements were done at 25 °C.

RESULTS

We found that at neutral pH, L-BABP displays a fluorescence emission spectrum that is typical for a Trp residue in a nonpolar environment. Besides, the far-UV−CD and IR spectra are in agreement with the known secondary structure (*2*), and the near-UV−CD spectrum reveals an anisotropic environment for the aromatic residues as expected for the native protein. When the pH decreases, several spectroscopic changes are observed. Together with the changes in the hydrodynamic radius measured by size exclusion chromatography, these observations indicate that L-BABP acquires compact, partly folded states at acidic pH. The spectroscopic and hydrodynamic characteristics of the native and the acidic states are the following.

Fluorescence Spectroscopy. The fluorescence emission of Trp is sensitive to the polarity of the medium and can be used as an effective detector for conformational changes in proteins. When excited selectively at 290 nm, it is the main contributor to the protein fluorescence (*10*). Chicken L-BABP has a single Trp residue located in β-strand A in position 6. In the native conformation, the indole lateral chain is pointing toward the inner cavity. Representative fluorescence emission spectra of L-BABP at different pHs and ionic strength are shown in Figure 1. At pH 7, both at high and low ionic strength, apo L-BABP shows spectra with a wavelength of maximum emission (λ_{max}) at 324 nm. This value indicates that the Trp residue in the native protein is located in a nonpolar environment (Chapter 11 in ref *10*). At pH 2.4 and low-salt concentration, the spectrum is red-shifted reaching a $\lambda_{max} = 344$ nm, indicating that the Trp residue is exposed to a more polar environment. When the pH is further decreased to 1−1.5 or the ionic strength increased to 0.1 M NaCl at pH 2.4, the spectra display the shape and position of the spectrum for the native protein, indicating that Trp senses a nonpolar environment (Figure 1). This observation strongly suggests that under these conditions L-BABP has a collapsed structure in which the Trp residue is hidden from the solvent. Similar changes in the fluorescence emission spectra as a function of pH have been described for several proteins (*11*, *12*). In those cases, the native fluorescence spectrum observed in acidic conditions is due to the acquisition of a native-like conformation. Following those reports, and according to the findings of the present work, we will refer to the states observed at around pH 2.4, 0.1 M NaCl and around pH 1.5 at low ionic strength as "folded acidic states" of L-BABP. For comparison, the position of the spectrum of the unfolded protein in GuHCl was included in Figure 1.

To have an insight into the protein dynamics and the state of aggregation, we measured the anisotropy of the Trp fluorescence emission. The native protein at pH 7 showed an anisotropy value of 0.13. This is within the range expected for a Trp fluorophore inserted into a native, globular protein, with a molecular weight of 14 kDa like L-BABP. In this case, the fluorescence anisotropy is a measure of the rotation of the whole protein. At pH 2.5 and low ionic strength, the anisotropy value was 0.06; this indicates that at least the segment where the Trp is located undergoes an independent, rapid, and isotropic motion, characteristic of an unfolded protein. For the folded acidic states, we obtained an anisotropy value of 0.11, which is similar to the value for the native protein. This result suggests that the folded acidic states are not multimeric aggregates of compact monomers. If this were the case, we should have observed larger values for the anisotropy, closer to the maximum theoretical value of 0.4 (Chapter 5 in ref *10*).

Circular Dichroism. Far-UV−CD. We used far-UV−CD to study the secondary structure of L-BABP under native and acidic conditions. As expected according to the structure of L-BABP (*2*), the far-UV−CD spectrum at pH 7 shows two peaks at 215 and 195 nm corresponding to a protein with a high proportion of β-strands (*13*) (Figure 2). At pH 2.4 and low ionic strength, the spectrum shows a band at around 200 nm typical of the denatured, unfolded state (*13*). However, it conserves a high ellipticity at 215 nm which could be indicative of residual β-structure. Further decrease in the ellipticity can be obtained in GuHCl 2 M (Figure 2), indicating that this state still contains some secondary structure. Decreasing the pH below 2 or increasing the ionic strength at pH 2.5 produces a partial recovery of the native spectrum (Figure 2). The spectra of the folded acidic states of L-BABP indicate that they are not in a random-coil state.

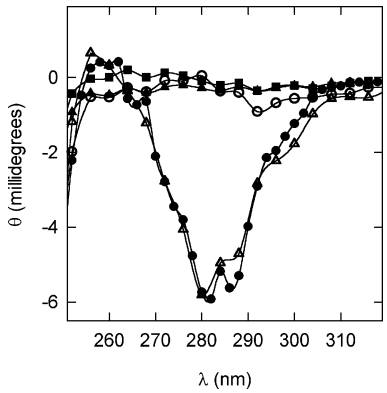

FIGURE 3: Near-UV−CD spectra of L-BABP at various pHs. (●) pH 7; (△) pH 4; (○) pH 1.5; (■) pH 2.5 no salt added; and (▲) pH 2.5 and 0.1 M NaCl.

Instead, they show some features of an α and *β* protein. The same spectral shape has been observed for an acidic partly folded state of tumor necrosis factor-α (*14*). For this protein, it was concluded that this spectral shape corresponds to a protein containing α-helix and *β*-chains.

Near-UV−CD. Changes in the tertiary structure of L-BABP due to the acidic conditions were studied using circular dichroism in the near-UV range; spectra are shown in Figure 3. L-BABP contains one Trp, six Phe, and two Tyr (*15*) that give rise to the spectrum in the near-UV region. At pH 7 and 4, the spectra display a band centered at 280 nm indicating the presence of a defined tertiary structure. The spectra are similar to that obtained by Schievano et al. (*16*). The absence of dichroism at pH 2.5 with no salt added, at 0.1 M NaCl (pH 2.5), and at pH 1.5 is indicative of the absence of a specific native environment for the side groups, that is, of the loss of tertiary structure, for these states.

Infrared Spectroscopy. The secondary structure of L-BABP in D_2O was studied at different pDs using infrared spectroscopy. The spectral components between 1750 and 1550 cm^{-1} were evidenced by the second derivatives of the original spectra and second derivatives of the Fourier self-deconvoluted spectra (*17*). To obtain the relative proportion of the components, we used a fitting procedure as in refs *18* and *7*. A Gaussian shape was assumed, and the components due to amino acid side chains (below 1600 cm^{-1} and above 1700 cm^{-1}) were included in the fitting. The area of the components obtained by this procedure can be considered proportional to the amount of the corresponding secondary structure present in the protein (*19*). Figure 4 shows the amide I′ spectra for L-BABP at pD 7.35, 2.10, and 1.35 (pD values indicate the direct reading of the glass electrode). The spectral components are summarized in Table 1.

At pD 7.25, the spectrum of L-BABP is characteristic of a protein with a large amount of *β*-structure and is composed of several bands as described previously (*7*). The bands centered at 1622 and 1632 cm^{-1} correspond to *β*-structures. Unordered structures generate the band at 1642 cm^{-1}. The band at 1652 cm^{-1} is assigned to α-helical structure. Components at 1661, 1670, 1680, and 1691 cm^{-1} arise from turns and bends, including *β*-turns. Bands at 1670 and 1680 cm^{-1} can also be assigned to extended *β*-structures. The total area corresponding to *β*-bands (1622, 1632 cm^{-1}) and α-helix (1652 cm^{-1}) comprise 50% and 14%, respectively, of the amide I' area. This is in good agreement with the number of residues in *β*-chains (58%) and α-helix (9%) observed for the native protein by X-ray crystallography (*2*).

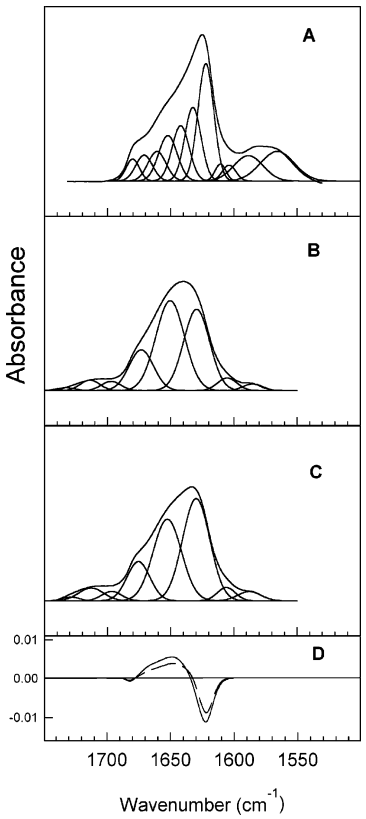

FIGURE 4: FTIR absorbance spectra of L-BABP at different pDs: (A) pD 7.25; (B) pD 2.10 no salt added; (C) pD 1.35. Gaussian curves below the spectra are the spectral components obtained by curve fitting. The positions of the components are displayed in Table 1. (D) Difference spectra obtained by subtracting a normalized spectrum at pD 7.25 from a normalized spectrum at pD 2.10 (continuous line) or at pD 1.35 (discontinuous line).

Decreasing the pD below 3 produces a large change in the shape of the FTIR spectra. At pD 2.1 (Figure 4), the spectrum is broader and clearly displays less structure. The second derivatives of both the Fourier self-deconvoluted and the normal (not self-deconvoluted) spectra show bands at 1627, 1651, and 1678 cm^{-1} (Figure 5). If the pD is decreased below 2, the spectrum displays more structure, although not to the same extent as observed at pD 7.25, and the bands corresponding to *β*-structures become more evident (Figures 4 and 5). Fourier self-deconvolution and second derivative revealed the same bands as obtained at pD 2.1 without salt (Figures 4 and 5 and Table 1). Fitting of the components to the original spectrum was performed according to the procedure described by Arrondo and Goñi (*19*). To obtain an acceptable fitting to the spectra at acidic pDs, the initial band positions obtained by self-deconvolution had to be allowed to shift from their positions (Table 1). The bandwidth also had to increase well above the value usually obtained for defined components in native proteins. These results strongly suggest that the band centered at 1651 cm^{-1} does not correspond only to α-helical structure but it also contains some proportion of other components such as unordered structures.

Difference spectra can also provide insight into the changes produced by a decreased pD. The subtraction of the spectra at acidic pDs from the spectrum at pD 7.25 is shown in

Table 1: Band Components of the FTIR Spectra

pD 7.25				pD 2.10				pD 1.35			
band position[a] (cm^{-1})	band position[b] (cm^{-1})	fwhh (cm^{-1})	% of the amide I′ band	band position[a] (cm^{-1})	band position[b] (cm^{-1})	fwhh (cm^{-1})	% of the amide I′ band	band position[a] (cm^{-1})	band position[b] (cm^{-1})	fwhh (cm^{-1})	% of the amide I′ band
1622.2	1622.3	14.8	30.3	1627	1629.6	24.3	37.2	1628.4	1629.9	25.3	46.3
1635	1632.5	15.1	19.5								
1640.7	1642.2	16	15.5								
1653.1	1652.3	17.4	13.9	1651.2	1650.5	26.7	45.2	1654.3	1652.7	26.3	38.3
1661	1661	16.8	8.8								
1670.5	1671.2	15.6	7.1	1678.4	1678.4	22.9	17.6	1677.5	1675.6	21.4	15.1
1680.7	1680.2	12.4	4.8								

[a] Band position (cm^{-1}) as detected by Fourier self-deconvolution and second derivative. [b] Band position (cm^{-1}) after curve fitting (see text). The assays were made in low ionic strength.

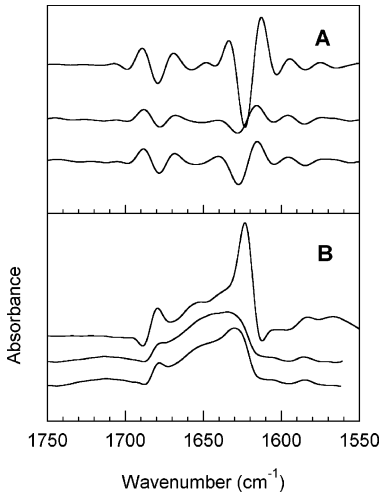

FIGURE 5: Second derivative of the FTIR deconvoluted spectra (A) and FTIR deconvoluted spectra using $K = 2$ and fwhh = 18 cm^{-1} (B). From top to bottom in each panel: pD 7.25, pD 2.10 no salt added, and pD 1.35.

Figure 4. The difference spectra show a negative band at 1625 cm^{-1} indicating a decrease of the content of β-structure in the acidic states and a wide positive band centered at 1650 cm^{-1} that can be interpreted as an increment in disordered and α-helical structures. This increment is clearly larger at pD 2.1 in the absence of salt than at pD 1.35.

Amide I′ bands below 1620 cm^{-1} are asigned to extended estructures in protein aggregates (*20*, *21*). We have not found these bands under acidic conditions whether at high or low ionic strength. This result indicates that there are no aggregates under acidic conditions.

The spectroscopic observations presented above indicate that at pH about 2.5, high ionic strength, or at pH 1.4, L-BABP is partly unfolded, retains a certain amount of secondary structure, and lacks stable tertiary structure. At pH 2.5, low ionic strength, the protein is even more unfolded, although retaining some secondary structure. To summarize and compare these global changes, we plotted several spectroscopic parameters as a function of the pH in Figure 6. We used the position of the center of mass (λ_{CM}) of the fluorescence emission spectra as a measurement of the position of the spectra. A red shift, or increase in λ_{max}, correlates with an increase in the λ_{CM}. We also included in Figure 6, (panel B) the fluorescence intensity measured at 320 nm. This is an extensive parameter that actually measures the degree of unfolding. The molar ellipticity at 215 nm was taken as a measurement of the amount of β-structure. Figure

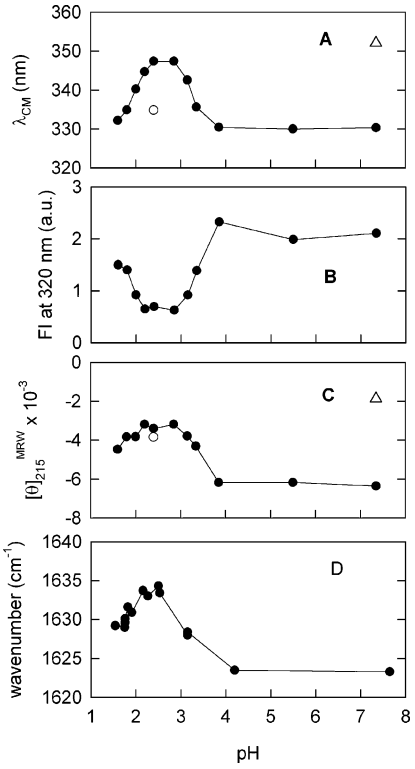

FIGURE 6: The pH dependence of spectroscopic parameters of L-BABP: (A) (●) position of center of mass of fluorescence emission, λ_{CM}, at low ionic strength, (○) λ_{CM} at high ionic strength, and (△) λ_{CM} in 2 M GuHCl; (B) (●) fluorescence intensity measured at 320 nm, low ionic strength; (C) (●) ellipticity measured at 215 nm, θ_{215}^{MRW}, at low ionic strength, (○) θ_{215}^{MRW} at high ionic strength, and (△) θ_{215}^{MRW} in 2 M GuHCl; (D) (●) position of the amide I′ IR band at low ionic strength.

6 also shows the wavenumber of maximum intensity of the IR spectra as a function of pH. Because the change in the shape of the amide I′ band is due to changes in their components, the band position can be considered as an overall index of secondary structure. It should be considered that, for the same H^+ or D^+ concentration, the glass electrode produces a reading 0.4 units lower in the deuterium oxide solution (*22*); the FTIR data in Figure 6 were corrected by this difference and can be directly compared with the experiments made in water.

The spectroscopic parameters plotted in Figure 6 remain constant between pH 7.4 and 4. A large exposure of Trp (increase in the value of λ_{CM}) and a loss of secondary structure (decrease of dichroic signal at 215 nm and shift of the IR spectra) occur within a narrow range between pH 4

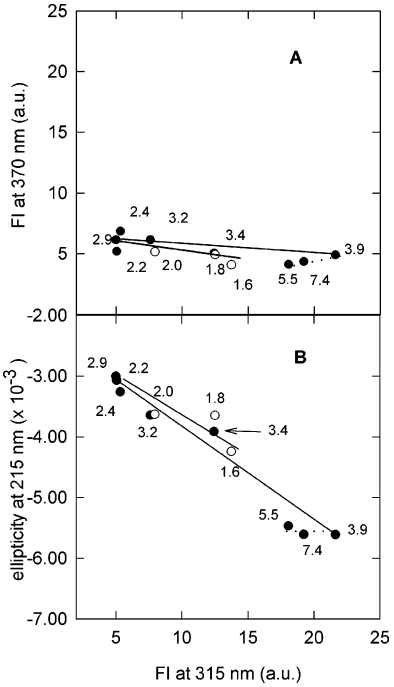

FIGURE 7: Phase diagram analysis of the spectroscopy changes in L-BABP induced by changes in pH. (A) Diagram based in fluorescence intensity at 370 nm vs fluorescence intensity at 315 nm. (B) Ellipticity at 215 nm vs fluorescence intensity at 315 nm. Numbers indicate the pH values for each data point. To highlight the changes that occur at low pH, points below pH 2.2 are in open symbols.

and 3−2.5, at low ionic strength. Further increase in the H^+ ion concentration produces a partial recovery of the native spectroscopic parameters also within few pH units. It must be taken into account that tertiary structure as measured by near-UV−CD (not shown in Figure 6) is only present in the pH range 7.4−4.

Phase Diagrams. To further study the occurrence of different states of L-BABP, we analized the parametric dependencies of the fluorescence and far-UV−CD spectra with the pH. The phase diagram method (*23*) is based on the simple fact that for a sample containing a mixture of species the spectral intensity at a given wavelength, $I(\lambda)$, is given by $I(\lambda) = \alpha_1 I_1(\lambda) + \alpha_2 I_2(\lambda)$. α_1 and α_2 are the fractions of molecules in the state 1 and 2; $I_1(\lambda)$ and $I_2(\lambda)$ are the intensities when the sample contains 100% of the molecules in the state 1 and 2, respectively. If we have a collection of spectra acquired under different experimental conditions (different pH values in our case) the following relationship can be demontrated: $I(\lambda_1) = a + (bI(\lambda_2))$ (*23*). It means that if a single equilibrium exists between species 1 and 2, which is shifted due to the change in the experimental conditions, a plot of espectral intensities measured at the wavelength λ_1 as a function of intensities at λ_2 must produce a straight line with slope *b* (see ref *23* for definition of *b*).

Figure 7A shows the dependence of the fluorescence intensity measured at 370 nm as a function of the intensity at 315 nm for a set of spectra taken at the different pH values. Three separate experiments produced similar results; the set of spectra used for Figure 7 are the same as for Figure 6.

A cluster of points at the right side in the diagram, (representative points are pHs 7.4, 5.5, and 3.9 in Figure 7), suggests a transition within this range. Compared with the point corresponding to pH 4, there is a significant tendency for the points between pH 7.4 and 5 to be located in a different region of the plane. Nevertheless, it is difficult to ascertain if this represents a real transition between two different states because other parameters such as the position of the fluorescence spectra, the near- and far-UV−CD, and IR spectra are constant between pH 7.4 and 4.

A clear transition is defined between pH 4 and 3 in Figure 7A, which corresponds with the large change in the position of fluorescence spectra shown in Figures 1 and 6. For the pH range 3−2.2, the points are in a cluster (left side in the diagram, Figure 7), indicating that the spectra are identical within this range. A well-defined transition occurs between pH 2.2 and 1.6. The line connecting the points in the left cluster with the points at low pH (pH 1.8, 1.6) has the same slope and overlay the line between the higher pHs and pH 3. The interpretation is that when decreasing the pH below 2.2, L-BABP tends to acquire the spectral characteristics of the native state.

A similar analysis performed in the far-UV−CD spectra (result not shown) revealed two well-defined transitions, one between pH 4 and pH 3 and the other between pH 2.2 and pH 1.6. In this analysis, the straight lines also overlaid, indicating that in the transition to pH 1.6 L-BABP has a tendency to acquire the native secondary structure. No transition was observed between pH 7 and 4.

The phase diagram method also produces useful information when the correlation between spectra of different nature is studied (*23*). Figure 7B shows the correlation between the changes in fluorescence and far-UV−CD as a function of pH. The diagram shows that between pH 4 and 3 and between 2.2 and 1.6 the changes in compactness, as measured by Trp fluorescence, occur together with changes in secondary structure. This plot also evidences that slight changes in fluorescence intensity occur between pH 7 and 4 without changes in the far-UV−CD spectra (dotted line at the right in the plot).

Size-Exclusion Chromatography. Molecular size exclusion chromatography can be used to study the hydrodynamic volume of proteins (*24*−*26*). Uversky (*27*) compiled data from several proteins and obtained the following relationship between the Stokes radius, Rs, and the molecular mass, *M*:

$$\log(\mathrm{Rs}) = -0.254 + 0.369 \log(M) \qquad (1)$$

We measured the apparent molecular mass of L-BABP under different conditions and estimated the Stokes radius (Rs) for the native, partly unfolded, and the unfolded states of L-BABP using eq 1. At pH 7, L-BABP eluted in a volume corresponding to 14 kDa (Rs = 18.9 Å) as expected for this protein in the native state.

For the folded acidic states (pH 2.5, high ionic strength, or pH 1.5, low ionic strength), we obtained an apparent *M* of 18 kDa and Rs = 20.7 Å. This represents an increment of 31% of the hydrodynamic volume, or 9.5% of the Rs, as compared with the native protein. This observation strongly suggest that these states have the characteristics of a molten globule (see section II in ref *29* and ref *28*).

At pH 2.5 without salt, L-BABP eluted with an apparent *M* of 27 kDa, which corresponds to an Rs = 24.1 Å. This is within the expected value for a protein of 14 kDa in the premolten globule state (*28*).

In agreement with the expected value for a protein of 14 kDa in the unfolded state (*27*), we obtained an apparent *M* of 56 kDa and Rs = 31.5 Å for L-BABP in the presence of 6 M GuHCl. The comparison of this value with the hydrodynamic radii observed for the acidic states clearly indicates that they have a compactness similar to the native state.

The results described above in the absence of GuHCl were obtained when L-BABP was loaded into the column at a 20 μM concentration. At pH 7 and pH 2.5 at low ionic strength, the K_d values remained constant up to a protein concentration of 300 μM. For the folded acidic states, the elution profiles were independent from the concentration in the range 20−80 μM. Above this range, the protein eluted in the void volume indicating the presence of soluble aggregates. We concluded that the blue-shifted fluorescence spectra observed for the folded acidic states, measured at a protein concentration of 7 μM, are due to the acquisition of compact monomeric structures, and they are not due to the insertion of Trp into a nonpolar environment generated within aggregates.

DISCUSSION

We found two partly folded states of apo L-BABP with well-defined spectroscopic and hydrodynamic characteristics under acidic conditions. One of these states resembles a molten globule while the other is a premolten globule-like state.

At pH 2.5, 0.1 M NaCl or below pH 2 and low ionic strength, Trp 6 is within an environment with a polarity similar to the native state. Also, the fluorescence anisotropy is similar to that measured in the native state indicating that the residue does not have the independent mobility expected for a random coil. The near-UV−CD spectra show that the aromatic residues are within an environment more isotropic that in the native state. They have a considerable amount of secondary structure as evaluated by far-UV−CD and FTIR spectroscopy of the amide I' band. The changes in CD and FTIR spectra are consistent with a decrease in β-structure and an increase in both α-helical and unordered structure as compared with the native state. These are compact states: their hydrodynamic radius are only 30% larger than that of the native protein. The acquisition of compact, partly folded states with native-like secondary structure under acidic conditions has been described for several proteins (*30*). In general, it is found that the excess of anions, whether from the added HCl at extremely low pH or from an added salt, produce the screening of the electrostatic interactions that destabilizes the unfolded state and allows the protein to refold (*31*).

There are several examples of proteins with high β-structure content (*32*) and all-β class proteins (*33*, *34*) that can adopt compact partly folded states. It is very interesting that in some cases (*35*, *36*) an increase in α-helix is observed as compared with the native structure. As proposed by Narhi et al. (*35*), this suggests that the long-range interactions established in the native fold determine the existence of a particular secondary structure. In the absence of these interactions, in the compact partly folded states, some segments fold according to their intrinsic propensities and acquire α-helical structures. Although the contribution of unfolded structures to the infrared band at 1650 cm^{-1} cannot be evaluated, it seems that for L-BABP, the amount of α-helix is also increased in the compact unfolded states.

As discussed by Dolgikh et al. for the molten globule of α-lactalbumin (*37*), the comparison between the results of fluorescence and near-UV−CD spectroscopy gives a clue to the extent and time scale of the fluctuations in the folded acidic states of L-BABP. The rotation of the whole molecule can account for the values of fluorescence anisotropy. Thus, if there are local fluctuations large enough to allow for independent Trp rotation, they are slower than 10^9 s^{-1} which is the time scale for fluorescence emission. The lack of dichroic absorption by the aromatic residues, which has a time scale of 10^{15} s^{-1}, reveals the existence of a large collection of states, separated by small energy barriers, with different symmetries for the environment of aromatic residues. Hence, we conclude that L-BABP in these acidic states fulfills one of the defined characteristics of the molten globule state (*29*): it is sufficiently unfolded to allow the averaging of the environment of the aromatic residues but not unfolded enough to allow for their free rotation as measured by Trp fluorescence anisotropy.

At pH values between 3 and 2 and low ionic strength, L-BABP acquires the characteristics of a premolten globule state. The red-shifted fluorescence spectra and the low value of fluorescence anisotropy indicate that the structure is more unfolded and fluctuating than in the acidic states described above. The peptide CD and infrared spectra also reveal less amount of secondary structure, although they do not correspond to the spectra of a random coil. Particularly, the infrared spectrum displays bands that clearly correspond to α-helix and β-strands. The size-exclusion chromatography showed that this state has an hydrodynamic volume about twice the volume of the native state, indicating that the number of native contacts is largely decreased. For this state, it can also be considered that the existence of secondary structure is strongly influenced by the intrinsic propensities of the amino acid sequence rather than by the compactness and long-range interactions.

The finding that L-BABP can exist as a partly unfolded structure in solution is relevant to understanding its mechanisms of interaction with lipid membranes. In a previous paper, we described that L-BABP binds to anionic lipid membranes acquiring a partly unfolded structure (*7*). We can now propose two simple, alternative mechanisms to explain those results: (i) the native protein has affinity for the anionic lipid membrane, and once it is bound, it undergoes a conformational change to the partially unfolded state and (ii) a small fraction of the protein is present in a partly unfolded state in solution which has affinity for the membrane, and the equilibrium is shifted to the bound, partly unfolded state in the presence of the anionic lipids. More information about this system is required to understand which of these mechanisms is actually working. Particularly, it is necessary to know if the postulated partly folded state does exist in solution. In general, protein unfolding at high H^+ ion concentration is due to the coupling between the folding reaction and a protonation reaction: if the unfolded state has more affinity or a larger number of sites for proton binding, the equilibrium must shift to this state at low pH (*38*). Then, the observation of a partly folded state at low pH leads us to conclude that it must also be present in the

solution at higher pH, even if not significantly populated. This species is a candidate for the intermediate that binds to the membrane. This proposal is reinforced if we consider that the interface of the negatively charged anionic lipid membrane is more acidic than the bulk solution (*39*). The low pH at the membrane interface could help to increase the concentration of the partly folded state and, as a consequence, the rate of membrane binding. We note that the infrared spectra observed in solution within a wide range of pH (this work) are different from those observed from the membrane-bound protein evidencing also that the interaction with the lipid is involved in determining the structural and thermodynamic state of membrane-bound L-BABP.

REFERENCES

1. Banaszak, L., Winter, N., Xu, Z., Bernlohr, D. A., Cowan, S., and Jones, T. A. (1994) Lipid-binding proteins: a family of fatty acid and retinoid transport proteins, *Adv. Protein Chem. 45*, 89−151.
2. Nichesola, D., Perduca, M., Capaldi, S., Carrizo, M. E., Righetti, P. G., and Monaco, H. L. (2004) Crystal structure of chicken liver basic fatty-acid binding protein complexed with cholic acid, *Biochemistry 43*, 14072−14079.
3. Peeters, R. A., Veerkamp, J. H., and Demel, R. A. (1989) Are fatty acid-binding proteins involved in fatty acid transfer?, *Biochim. Biophys. Acta 1002*, 8−13.
4. Spener, F., Börchers, T., and Mukherjea, M. (1989) On the role of fatty acid binding proteins in fatty acid transport and metabolism, *FEBS Lett. 244*, 1−5.
5. Kim, H. K., and Storch, J. (1992) Free fatty acid transfer from rat liver fatty-acid binding protein to phospholipid vesicles. Effect ligand and solution properties, *J. Biol. Chem. 267*, 77−82.
6. Kim, H. K., and Storch, J. (1992) Mechanism of free fatty acid transfer from rat heart fatty acid-binding protein to phospholipid membranes. Evidence for a collisional process, *J. Biol. Chem. 267*, 20051−20056.
7. Nolan, V., Perduca, M., Monaco, H. L., Maggio, B., and Montich, G. G. (2003) Interactions of chicken liver fatty acid-binding protein with lipid membranes, *Biochim. Biophys. Acta 1611*, 98−106.
8. Pinheiro, T. J. T., Elöve, G. A., Watts, A., and Roder, H. (1997) Structural and kinetic description of cytochrome *c* unfolding induced by the interaction with lipid vesicles, *Biochemistry 36*, 13122−13132.
9. Scapin, G., Spadon, P., Pengo, L., Mammi, M., Zanotti, G., and Monaco, H. L. (1988) Chicken liver fatty acid-binding protein (pI = 9). Purification, crystallization and preliminary X-ray data, *FEBS Lett. 240*, 196−200.
10. Lakowicz, J. R. (1983) *Principles of Fluorescence Spectroscopy*, Plenum Press, New York.
11. Goto, Y., Calciano, L. J., and Fink, A. L. (1990) Acid-induced folding of proteins, *Proc. Natl. Acad. Sci. U.S.A. 87*, 573−577.
12. Kuwajima, K. (1989) The molten globule state as a clue for understanding the folding and cooperativity of globular proteins structure, *Proteins: Struct., Funct., Genet. 6*, 87−103.
13. Venyaminov, Y. S., and Yang J. T. (1996) Determination of protein secondary structure, in *Circular Dichroism and the Conformational Analysis of Biomolecules* (Fasman, G. D., Ed.) pp 69−107, Plenum Press, New York and London.
14. Narhi, L. O., Philo, J. S., Li, T., Zhang, M., Samal, B., and Arakawa, T. (1996) Induction of α-helix in the *β*-sheet protein tumor necrosis factor-α: acid-induced denaturation, *Biochemistry 35*, 11454−11460.
15. Ceciliani, F., Monaco, H. L., Ronchi, S., Faotto, L., and Spadon, P. (1994) The primary structure of a basic (pI 9.0) acid-binding protein from liver of *Gallus domesticus*, *Comp. Biochem. Physiol. B109*, 261−271.
16. Schievano, E., Quarzago, D., Spadon, P., Monaco, H. L., Zanotti, G., and Peggion, E. (1994) Conformational and binding properties of chicken liver basic fatty acid binding protein in solution, *Biopolymers 24*, 879−887.
17. Arrondo, J. L. R., Muga, A., Castresana, J., and Goñi, F. M. (1993) Quantitative studies of the structure of proteins in solution by Fourier transform infrared spectroscopy, *Prog. Biophys. Mol. Biol. 59*, 23−56.
18. Chehin, R., Iloro, I., Marcos, M. J., Villar, E., Shnyrov, V. L., and Arrondo, J. L. R. (1999) Thermal and pH-induced conformational changes of a *β*-sheet protein monitored by infrared spectroscopy, *Biochemistry 38*, 1525−1530.
19. Arrondo, J. L. R., and Goñi, F. M. (1999) Structure and dynamics of membrane proteins as studied by infrared spectroscopy, *Prog. Biophys. Mol. Biol. 72*, 367−405.
20. Surewicz, W. K., Leddy, J. J., and Mantsch, H. H. (1990) Structure, stability, and receptor interaction of cholera toxin as studied by Fourier transform infrared spectroscopy, *Biochemistry 29*, 8106−8111.
21. Arrondo, J. L., Castresana, J., Valpuesta, J. M., and Goñi, F. M. (1994) Structure and thermal denaturation of crystalline and noncrystalline cytochrome oxidase as studied by infrared spectroscopy, *Biochemistry 33*, 11650−11655.
22. Glasoe, P. K., and Long, F. A. (1960) Use of glass electrodes to measure acidities in deuterium oxide, *J. Phys. Chem. 64*, 188−190.
23. Kuznetsova, I. M., Turoverov, K. K., and Uversky, V. N. (2004) Use of the phase diagram method to analyze the protein unfolding-refolding reactions: fishing out the "invisible" intermediates, *J. Proteome Res. 3*, 485−494.
24. Ackers, G. K. (1967) A new calibration procedure for gel filtration columns, *J. Biol. Chem. 242*, 3237−3238.
25. Ackers, G. K. (1970) Analytical gel chromatography of proteins, *Adv. Protein Chem. 24*, 343−446.
26. Corbett, R. J. T., and Roche, R. S. (1984) Use of high-speed size-exclusion chromatography for the study of protein folding and stability, *Biochemistry 23*, 1888−1894.
27. Uversky, V. N. (1993) Use of fast protein size-exclusion liquid chromatography to study the unfolding of proteins which denature through the molten globule, *Biochemistry 32*, 13288−13298.
28. Uversky, V. N. (2002) Natively unfolded proteins: a point where biology waits for physics, *Protein Sci. 11*, 739−756.
29. Ptitsyn, O. B. (1995) Molten globule and protein folding, *Adv. Protein Chem. 47*, 83−229.
30. Fink, A. L., Calciano, L. J., Goto, Y. Kurotsu, T., and Palleros, D. (1994) Clasification of acid denaturation of proteins: intermediates and unfolded states, *Biochemistry 33*, 12504−12511.
31. Goto, Y., Takahashi, N., and Fink, A. L. (1990) Mechanism of acid-induced folding of proteins, *Biochemistry 29*, 3480−3488.
32. Vassilenko, K. S., and Uversky, V. N. (2002) Native-like secondary structure of molten globules, *Biochim. Biophys. Acta 1594*, 168−177.
33. Sivaraman, T., Kumar, T. K. S., Jayaraman, G., Han, C. C., and Yu, C. (1997) Characterization of a partially structured state in an all-*β*-sheet protein, *Biochem. J. 321*, 457−464.
34. Samuel, D., Kumar, T. K. S., Srimathi, T., Hsieh, H., and Yu, C. (2000) Identification and characterization of an equilibrium intermediate in the unfolding pathway of an all *β*-barrel protein, *J. Biol. Chem. 275*, 34968−34975.
35. Narhi, L. O., Philo, J. S., Li, T., Zhang, M., Samal, B., and Arakawa, T. (1996) Induction of α-helix in the *β*-sheet protein tumor necrosis factor-α: thermal and trifluoroethanol-induced denaturation at neutral pH, *Biochemistry 35*, 11447−11453.
36. Forge, V., Hoshino, M., Kuwata, K., Arai, M., Kuwajima, K., Batt, C., and Goto, Y. (2000) Is folding of *β*-lactoglobulin non-hierarchic? Intermediate with native-like *β*-sheet and non-native α-helix, *J. Mol. Biol. 296*, 1039−1051.
37. Dolgikh, D. A., Gilmanshin, R. I., Brazhnikov, E. V., Bychkova, V. E., Semisotnov, G. V., Venyaminov, Y. S., and Ptitsyn, O. B. (1981) α-Lactalbumin: compact state with fluctuating tertiary structure?, *FEBS Lett. 136*, 311−315.
38. Wyman, J., and Gill, S. J. (1990) *Binding and Linkage: Functional Chemistry of Biological Macromolecules*, University Science Books, Mill Valley, CA.
39. McLaughlin, S. (1989) The electrostatic properties of membranes, *Annu. Rev. Biophys. Biophys. Chem. 18*, 113−136.

BI050129R